



Plantaricin A, a cationic peptide produced by *Lactobacillus plantarum*, permeabilizes eukaryotic cell membranes by a mechanism dependent on negative surface charge linked to glycosylated membrane proteins

Sverre L. Sand, Jon Nissen-Meyer, Olav Sand, Trude M. Haug*

Department of Molecular Biosciences, University of Oslo, Oslo, Norway

ARTICLE INFO

Article history:

Received 19 April 2012

Received in revised form 1 October 2012

Accepted 1 November 2012

Available online 8 November 2012

Keywords:

Antimicrobial peptide

Electrophysiology

Ca²⁺ imaging

Electrostatic attraction

Cancer cell

Cell lysis

ABSTRACT

Lactobacillus plantarum C11 releases plantaricin A (PlnA), a cationic peptide pheromone that has a membrane-permeabilizing, antimicrobial effect. We have previously shown that PlnA may also permeabilize eukaryotic cells, with a potency that differs between cell types. It is generally assumed that cationic antimicrobial peptides exert their effects through electrostatic attraction to negatively charged phospholipids in the membrane. The aim of the present study was to investigate if removal of the negative charge linked to glycosylated proteins at the cell surface reduces the permeabilizing potency of PlnA. The effects of PlnA were tested on clonal rat anterior pituitary cells (GH₄ cells) using patch clamp and microfluorometric techniques. In physiological extracellular solution, GH₄ cells are highly sensitive to PlnA, but the sensitivity was dramatically reduced in solutions that partly neutralize the negative surface charge of the cells, in agreement with the notion that electrostatic interactions are probably important for the PlnA effects. Trypsination of cells prior to PlnA exposure also rendered the cells less sensitive to the peptide, suggesting that negative charges linked to membrane proteins are involved in the permeabilizing action. Finally, pre-exposure of cells to a mixture of enzymes that split carbohydrate residues from the backbone of glycosylated proteins also impeded the PlnA-induced membrane permeabilization. We conclude that electrostatic attraction between PlnA and glycosylated membrane proteins is probably an essential first step before PlnA can interact with membrane phospholipids. Deviating glycosylation patterns may contribute to the variation in PlnA sensitivity of different cell types, including cancerous cells and their normal counterparts.

© 2012 Elsevier B.V. All rights reserved.

1. Introduction

Nearly all organisms produce antimicrobial peptides, for review see [1–4]. Some antimicrobial peptides from insects [5,6], amphibians [7,8], and mammals [9,10] also kill a variety of tumor cells at concentrations not affecting normal eukaryotic cells, indicating a possible therapeutic potential of such peptides (reviewed in [11]).

Antimicrobial peptides produced by bacteria, i.e., bacteriocins, are usually more specific in their actions, and generally do not affect eukaryotic cells. However, we have recently shown that the antimicrobial peptide plantaricin A (PlnA), which is produced by *Lactobacillus plantarum* C11, may permeabilize eukaryotic cells with a potency that differs between cell types [12–14]. PlnA is primarily a peptide pheromone that induces bacteriocin production in the strain from

which it is released [15,16]. However, the peptide also has membrane-permeabilizing strain-specific antimicrobial activity [17,18].

Upon contact with the membrane, PlnA interacts with the membrane lipids in a non-chiral manner, forming an α -helical structure before binding to the receptor that induces the pheromone effect [19]. The antimicrobial activity against sensitive bacterial strains is probably linked to the initial membrane-interacting step.

In our first study of membrane permeabilization of eukaryotic cells induced by PlnA, we found that both the L- and D-form of PlnA (10 μ M) caused massive membrane permeabilization within seconds in the cancerous rat pituitary GH₄ cell line, while primary cell cultures of rat anterior pituitary were insensitive to the peptide (1 mM) [13]. Unfortunately, later studies on other cell types showed that the effect of PlnA is not restricted to cancerous cells [12,14]. However, Berge et al. [20] have recently shown that high selectivity for cancer cells is not an absolute requirement for utilizing lytic peptides in cancer treatment. In these experiments, a lytic peptide derived from lactoferrin was injected intratumorally. This treatment not only eradicated tumors by local cell lysis, but more importantly also through induction of specific immunity against all cells from the same clone as the lysed cells. Similar results from treatment with oncolytic viruses, which activate a

* Corresponding author at: Department of Molecular Biosciences, University of Oslo, Post box 1041 Blindern, N-0316 Oslo, Norway. Tel.: +47 844414, +47 92855894; fax: +47 22857655.

E-mail addresses: sverre.sand@medisin.uio.no (S.L. Sand), jon.nissen-meyer@imbv.uio.no (J. Nissen-Meyer), olav.sand@imbv.uio.no (O. Sand), t.m.haug@imbv.uio.no (T.M. Haug).

systemic immune response by lysis of tumor cells, have previously been reported [21,22]. These results have instigated further investigation of PlnA's mode of action.

Most antimicrobial peptides are cationic and amphiphilic or hydrophobic, and their antimicrobial effect is mainly due to membrane permeabilization. It is generally assumed that electrostatic attraction to negatively charged phospholipids facilitates the peptide's initial interaction with the cell surface, whereas their amphiphilic or hydrophobic properties enables membrane insertion [18]. The molecular mechanisms for the lytic effects are still not completely understood, and suggested modes of action range from formation of distinct or variable transmembrane pores to detergent-like effects on the membrane [23–31]. PlnA's mode of action is probably in the latter category [13].

In all cells, the various phospholipids are asymmetrically distributed between the two membrane leaflets. Bacteria keep most of their negatively charged phospholipids in the outer membrane leaflet, whereas eukaryotic cells keep most of theirs, particularly phosphatidylserine, in the inner leaflet by means of specific, energy-requiring transporters (reviewed in [32]). Consequently, cationic antimicrobial peptides usually fail to permeabilize eukaryotic cell membranes [33–36]. However, in cancerous and damaged cells, the density of negatively charged phospholipids in the outer membrane leaflet is somewhat increased [37–40], which is a favored explanation for why some antimicrobial peptides permeabilize cancerous eukaryotic cells (reviewed in [11]).

In conflict with this hypothesis, we have previously shown that the inner leaflet of the cell membrane of pituitary cells is resistant to PlnA [13], indicating that negatively charged macromolecules associated with the outer membrane leaflet may be essential for the permeabilizing effect of PlnA. Glycosylated membrane proteins, which are important components of the juxtamembrane environment, constitute a major group of such macromolecules. These membrane proteins are structurally divided into glycoproteins, with relatively short, branched or unbranched glycan side chains, and proteoglycans, which are heavily glycosylated with glycosaminoglycans (GAGs). These are negatively charged, long, unbranched polysaccharides consisting of a single repeating disaccharide unit. The properties of this polymeric material coating all cells are highly diverse and vary between tissues and individuals. Interestingly, synthesis of proteoglycans is dramatically altered during neoplastic transformation, and overexpression of various subtypes has been shown in numerous malignancies [41–48]. Moreover, marked structural alterations of GAG sidechains have also been recorded [49–51].

We have previously suggested that electrostatic attraction to negatively charged membrane-associated macromolecules may facilitate membrane insertion of PlnA by ensuring a relatively high local concentration of the peptide close to the lipid bilayer [12–14]. The aim of the present study was to examine if glycosylated membrane proteins may be involved in such a mechanism, which might also explain the variation in PlnA sensitivity among different cell types, and between neoplastic cells and their normal counterparts. We have investigated the effect of PlnA on GH₄ cells, the clonal cell line previously shown to be highly sensitive to PlnA [13], after various manipulations of cell surface charge and composition of glycosylated membrane proteins. Membrane permeabilization was monitored by measuring membrane conductance and changes in the cytosolic Ca²⁺ concentration. The results suggest that electrostatic attraction between PlnA and glycosylated membrane proteins is an essential first step for PlnA-induced membrane permeabilization and cell lysis.

2. Materials and methods

2.1. Synthesis and purification of PlnA

Both the L- and D-enantiomeric forms of the 22-mer version of PlnA were synthesized according to the amino acid sequence of the

peptide [15]: Tyr-Ser-Leu-Gln-Met-Gly-Ala-Thr-Ala-Ile-Lys-Gln-Val-Lys-Lys-Leu-Phe-Lys-Lys-Trp-Gly-Trp. The natural L-form of PlnA-22 was purchased from GenScript (Piscataway, NJ, USA), at a purity of more than 90%. The D-enantiomer was synthesized locally, and purified according to the method previously described [17]. The absorbance at 280 nm was measured, and the peptide concentration was calculated using the molar extinction coefficient at this wavelength. The coefficient at 280 nm is 12,660 M⁻¹ cm⁻¹ in 6.0 M guanidinium hydrochloride, 0.02 M phosphate buffer, pH 6.5, as deduced from PlnA's amino acid composition [16]. The net charge of the peptide is approximately +5 at neutral pH. In a separate, ongoing study, the effects of both amino acid substitutions and peptide truncations on the permeabilizing effect of PlnA is explored. Several of the substitutions and truncations reduce or abolish the permeabilizing effects of PlnA. For example, substitution of each one of the following amino acids with proline virtually abolishes the membrane permeabilizing effect of PlnA: valine-13, leucine-16 and phenylalanine-17 (residue #1 is N-terminal tyrosine). Thus, the membrane permeabilizing ability of PlnA is sequence-specific.

2.2. Culture of clonal rat anterior pituitary cells

The GH cell lines were originally derived from a rat pituitary tumor [52]. These cells spontaneously synthesize and secrete prolactin and/or growth hormone and are electrically excitable. In the present study, we used the prolactin-secreting GH₄C₁ cell line. Cells were grown as monolayer cultures in plastic tissue culture flasks containing Ham's F-10 medium supplemented with horse serum (7.5%), fetal calf serum (2.5%), penicillin (50 U mL⁻¹), and streptomycin (100 µg mL⁻¹) at 37 °C in a humidified atmosphere of 5% CO₂ and 95% air. Cells were seeded in 35 mm plastic dishes 3–7 days prior to recording. In order to harvest cells from the culture flask, the normal growth medium was replaced with Ca²⁺-free (EDTA) saline containing 200 mg/L trypsin (Lonza, Verviers, Belgium). The trypsin solution was removed after 1 min, followed by 3 min incubation to allow detachment of the cells. The cells were then suspended in growth medium, centrifuged for 3 min at 100 g, and resuspended in growth medium before being seeded at a density of 150,000 cells/cm². For microfluorometric experiments, the cells were seeded in similar dishes fitted with a central glass bottom 14 mm in diameter. For Ca²⁺ imaging experiments, a circular border of silicone was applied around the glass bottom, thus forming a perfusion chamber with a volume of approximately 0.6 mL. All experiments were carried out at room temperature.

2.3. Experimental solutions

The physiologically adapted extracellular solution, hereafter called "normal extracellular solution", contained (mM): 150 NaCl, 5 KCl, 2.4 CaCl₂, 1.3 MgCl₂, 10 glucose, 10 HEPES/NaOH (pH 7.4). For the experiments performed in isotonic solution with high extracellular Ca²⁺ concentration, CaCl₂ and NaCl concentrations were altered to 24 mM and 118 mM, respectively. In these experiments, the solution with elevated Ca²⁺ concentration was introduced 3–5 min prior to the recordings. Patch electrodes were filled with the following solution (mM): 120 CH₃SO₃K, 20 KCl, 10 HEPES/NaOH, 20 sucrose (pH 7.2). Poly-D-lysine hydrobromide (PDL) (Sigma, St. Louis, MO, USA) was dissolved in normal extracellular solution to a concentration of 5 mg/ml.

2.4. Enzyme treatment

Trypsin treatment of cells was performed with various concentrations of trypsin, based on a solution of 25 g porcine trypsin/L in 0.9% NaCl (Sigma, MO, USA). Enzymes affecting glycosylated membrane proteins were dissolved in a buffered solution that contained (mM): 150 NaCl, 5 KCl, 2.4 CaCl₂, 1.3 MgCl₂, 10 glucose, 5.5 CH₃COONa, 10

HEPES/NaOH, (pH 7.0). The following enzyme amounts (mU) were mixed together in 1.5 ml buffer: 200 chondroitinase ABC (cABC) (Seikagru corp., Tokyo, Japan), 150 N-Glycosidase F (PNGase F) (Roche, Mannheim, Germany), 0.25 heparinase I, II, II (Grampian Enzymes, Orkney Islands, UK). Cells were incubated in the enzyme mixture three hours prior to experiments.

2.5. Electrophysiology

Outside-out patch clamp recordings were used to directly monitor the effects of PlnA on the membrane conductance, which mirrors the membrane permeability. The patch electrodes were made from borosilicate glass with filament and fire-polished before use, and the electrode resistance was 3–6 M Ω . The electrodes were connected to an EPC-7 patch-clamp amplifier (Heka, Lambrecht/Pfaltz, Germany) controlled by the software PClamp 9.2 (Axon Instruments, Union City, CA, USA). The recorded signals were digitized at 10 kHz, filtered at 3 kHz and stored on a computer. Recordings were not adjusted for the electrode junction potentials. Membrane currents flowing from the extracellular to the intracellular side were defined as negative and displayed as downward deflections in the current traces. Data analysis was performed using PClamp 9.2 and Origin 7.0 (OriginLab, Northampton, MA, USA). The excised patches were exposed to PlnA by pressure ejection (about 1 kPa) from a micropipette (inner tip diameter 1–2 μ m) placed about 40 μ m from the excised patch. No artifacts were observed when ejecting normal extracellular solution onto patches from this distance. Patches were pretreated for 1 min with poly-D-lysine (5 mg/L in normal EC) or trypsin (25 g/L in 0.9% NaCl) by placing the patch within the orifice of the approximately 10 μ m tip of a micropipette containing the treatment solution. The micropipette was filled up to a level about 1 cm above that sustained by capillary action, thus securing a small and even outward flow of solution flushing the patch. No artifacts were observed during this pretreatment. Before exposure to PlnA, the PDL- or trypsin-containing pipette was withdrawn from the bath.

2.6. Microfluorometry of fura-2-loaded cells

The cells were loaded with the fluorescent Ca^{2+} indicator fura-2 by exposure to 5 μ m fura-2/AM (Invitrogen, Carlsbad, CA, USA) in extracellular solution for 40 min at 37 $^{\circ}\text{C}$, followed by washout of the fura-2 ester and further 30 min incubation at room temperature. For Ca^{2+} imaging, an Olympus IX71 inverted microscope with objectives of high UV light transmittance was used (Olympus, Tokyo, Japan). A Lambda 10–2 filter wheel (Sutter, CA, USA) switched the excitation light from a Lambda LS Xenon Arc Lamp (Sutter, CA, USA) between 340 and 380 nm, while the emitted fluorescence was recorded at 510 nm. The exposure times varied between 100 and 300 ms for 340 nm and between 50 and 150 ms for 380 nm, depending on the degree of cell loading with fura-2. The ratio between emissions at these excitation wavelengths (F340/F380) reflects the cytosolic Ca^{2+} concentration ($[\text{Ca}^{2+}]_i$). Fluorescence images were captured by a Hamamatsu ORCA ER camera (Hamamatsu Photonics, Hamamatsu, Japan), and ratio images were obtained at a frequency of 0.67 Hz. For controlling the hardware and storing and analyzing the data, the software Imaging Workbench 5.2 (Indec Systems, CA, USA) was used. The digitized data were background-subtracted, and the relative $[\text{Ca}^{2+}]_i$ concentrations were displayed by pseudo colors. In the present study, the relative increase in $[\text{Ca}^{2+}]_i$ is used as an indirect measure of reduced cell membrane integrity. Therefore, calibration in order to determine the absolute Ca^{2+} concentrations was not performed. Recording sessions lasted less than 5 min, and photobleaching or phototoxicity did not pose a problem within this time span. The liquid volume in the perfusion chamber was kept at 150–200 μ l by applying continuous suction through a narrow tube appropriately positioned relative to the preferred surface level. PlnA was applied by flushing the chamber with 400–600 μ l of peptide-containing solution.

The chamber perfusion used in the set-up for Ca^{2+} imaging requires firm attachment of the cells to the bottom of the dish. However, in the experiments testing the effects of PlnA on trypsinated cells, the enzyme treatment partially detached the cells from the bottom of the dish. In these experiments, we therefore recorded changes of $[\text{Ca}^{2+}]_i$ in single cells fixed by a suction micropipette, and the fluorescence from the selected cell was measured using a photomultiplier tube. The dish with fura-2-loaded cells was then mounted on an Olympus IMT-2 inverted microscope, forming the central part of the Olympus OSP-3 system for dual excitation fluorometry (Olympus, Tokyo, Japan). The excitation light was switched at 200 Hz between 360 and 380 nm using a rotating mirror. The emitted fluorescence was recorded at 510 nm and the measurements were restricted to a single cell by a pinhole diaphragm. Whereas the ratio F360/F380 reflects $[\text{Ca}^{2+}]_i$, the emission at the isosbestic wavelength 360 nm is independent of $[\text{Ca}^{2+}]_i$, and thus monitors the cytosolic concentration of the fluorophore. Prior to experiments, the normal extracellular solution was replaced with trypsin-containing solution obtained by diluting the 25 g trypsin L^{-1} stock solution with normal extracellular solution to a final trypsin concentration of 250 mg L^{-1} . The cells were incubated at room temperature for 3–5 min before the first recording. The cells were then either detached from the bottom or only partially adherent. For each recording, a selected cell was therefore fixed by a suction micropipette (suction about -5 kPa) with a tip diameter of about 4 μ m, and the cell was exposed to PlnA by pressure ejection as described in Section 2.5.

3. Results

3.1. Neutralization of negative surface charges prevents membrane permeabilization by PlnA

The assumption that electrostatic interactions are essential for the membrane-permeabilizing effect of PlnA was tested by exposing cells with reduced surface charge to the peptide. The negative surface charge of cells can easily be partially neutralized by elevating the extracellular concentration of polyvalent cations, e.g. Ca^{2+} , or adding organic compounds with excess positive charge, e.g. poly-D-lysine, to the extracellular solution. Therefore, in this series of experiments, the permeabilizing effect of 10^{-4} M PlnA was studied on cells exposed to either 24 mM Ca^{2+} or 5 mg/ml poly-D-lysine. At this concentration of PlnA, the cell membrane of GH₄ cells in normal extracellular solution is rapidly disrupted [13].

Fig. 1 shows representative recordings from outside-out patches voltage clamped at -50 mV during exposure to 10^{-4} M PlnA. The recording in Fig. 1A was obtained in normal extracellular solution, and PlnA was applied by pressure ejection directly onto the patch. Within less than 5 s, the peptide induced a rapidly increasing inward current, reflecting pronounced membrane permeabilization. However, in solutions with 24 mM Ca^{2+} (Fig. 1B) or containing 5 mg/ml poly-D-lysine (Fig. 1C), PlnA failed to permeabilize the membrane. The recordings started about 5 min after replacement of the normal extracellular solution in the dish with the test solution, and the patches were exposed to 10^{-4} M PlnA for at least 3 min. In the 13 recordings obtained in solution with elevated Ca^{2+} concentration and the 12 recordings acquired in solution containing poly-D-lysine, the holding current was virtually stable throughout the recording period in 11 and 9 of the recordings, respectively. In order to confirm the potency of PlnA, control recordings in normal extracellular solution were performed at regular intervals, and all of the 18 control patches were readily permeabilized by 10^{-4} M PlnA.

3.2. Ca^{2+} imaging confirms the dependence of negative surface charge for the effect of PlnA

The results from the patch-clamp experiments were verified by Ca^{2+} imaging, as shown in Fig. 2 for cells exposed to elevated Ca^{2+}

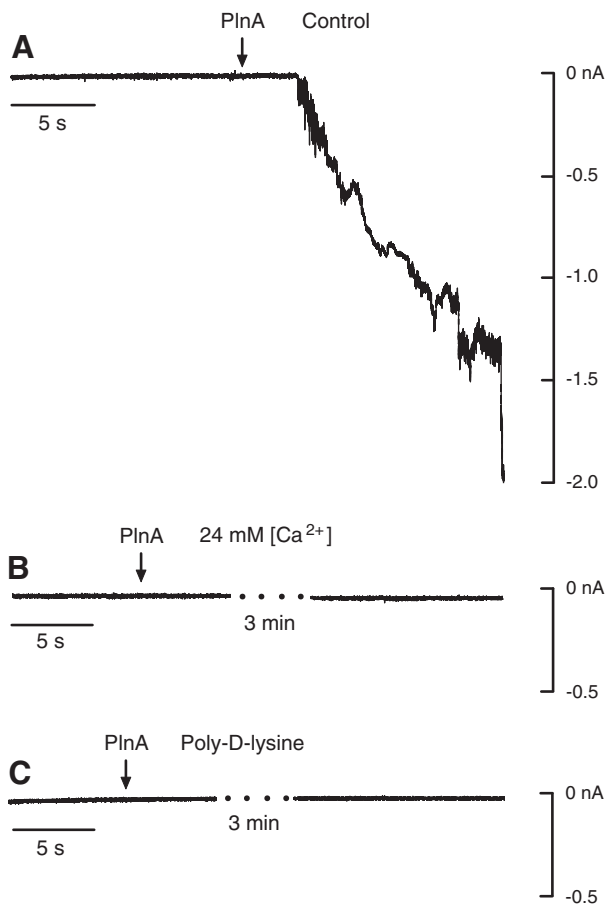


Fig. 1. Neutralization of negative surface charges inhibits membrane permeabilization by PInA. Representative recordings from outside-out patches voltage clamped at -50 mV are displayed. Arrows indicate start of continuous pressure ejections of 10^{-4} M PInA onto the patches. (A) The peptide permeabilized the membrane in normal extracellular solution, as shown by the induced membrane current. In extracellular solutions that neutralize negative surface charges, i.e., with $10\times$ increased Ca^{2+} concentration (24 mM) (B) or 5 mg/ml poly-D-lysine (C), 10^{-4} M PInA failed to permeabilize the membrane.

concentration and in Fig. 3 for cells in solution containing poly-D-lysine. The ratio images of fura-2-loaded cells in these figures display relative $[\text{Ca}^{2+}]_i$ by pseudo colors, where dark blue represents resting levels and dark red indicates saturating levels of $[\text{Ca}^{2+}]_i$. Figs. 2A and 3A show cells from two different seedings in normal extracellular solution. The frames are separated by 5 s, and the first image in each panel was taken immediately before the cell chamber was flushed with solution containing 10^{-4} M PInA. Already in the second image of each panel, i.e., less than 5 s after exposure to PInA, some of the cells displayed an obvious color shift showing a rapid increase of $[\text{Ca}^{2+}]_i$. Within 20–25 s, nearly all cells in the field of view reached saturating levels of $[\text{Ca}^{2+}]_i$, suggesting increased Ca^{2+} influx due to membrane permeabilization.

Fig. 2B presents a similar experiment on cells in solution with $10\times$ increased Ca^{2+} concentration (24 mM). The time interval between the merged frames is 5 s, while the last, separated frame was taken 3 min after start of PInA exposure. Whereas cells were clearly permeabilized by 10^{-4} M PInA in normal extracellular solution in less than 20–25 s (Fig. 2A), the $[\text{Ca}^{2+}]_i$ of cells in the solution with elevated Ca^{2+} concentration was seemingly rather stable, even after 3 min exposure to 10^{-4} M PInA (Fig. 2B). This series of experiments comprised 5 control dishes with normal extracellular solution and 6 dishes containing solution with 24 mM Ca^{2+} concentration. Control recordings were performed at regular intervals during the experiments, in order to test the potency of PInA on cells from this

particular seeding. In all the control dishes with normal extracellular solution, the cells displayed pronounced elevation of $[\text{Ca}^{2+}]_i$ within less than 30 s in response to 10^{-4} M PInA. In the control experiments, the F340/F380 ratio of the observed cells increased by a factor of 4.8 ± 1.1 (S.D., $n = 100$) after 30 s exposure to 10^{-4} M PInA. However, in the solution with elevated Ca^{2+} concentration, the F340/F380 ratio of the recorded cells increased by a factor of only 1.2 ± 0.2 ($n = 110$) after 3 min exposure to 10^{-4} M PInA. This difference in ratio increase between the two experimental situations is highly significant (Student t-test, $p < 0.0001$).

In a corresponding series of experiments, the effect of 10^{-4} M PInA was also studied on cells in extracellular solution containing 5 mg/ml poly-D-lysine (Fig. 3B), and the result was essentially the same as that described for cells in solution with 24 mM Ca^{2+} . In these experiments, 4 control dishes with normal extracellular solution and 4 dishes containing solution with 5 mg/ml poly-D-lysine were included. In all the dishes with normal extracellular solution, 10^{-4} M PInA induced pronounced elevation of $[\text{Ca}^{2+}]_i$ within less than 30 s in virtually all the cells. The F340/F380 ratio of the control cells increased by a factor of 4.3 ± 1.3 ($n = 46$) after 30 s exposure to 10^{-4} M PInA. In contrast, the F340/F380 ratio of cells in solution containing poly-D-lysine increased to only 1.2 ± 0.1 ($n = 33$) after 3 min exposure to 10^{-4} M PInA, and this value is significantly less than the ratio increase in the control cells ($p < 0.0001$).

The conclusion from both the patch clamp and the Ca^{2+} imaging experiments is that electrostatic interaction between the cationic PInA molecule and the negative surface charge of the cell is probably an essential step in the membrane-permeabilizing action of PInA.

3.3. Trypsin-treated cells are resistant to PInA

Although the experiments described in the previous sections demonstrate that negative surface charges are involved in the membrane-permeabilizing effect of PInA, they do not reveal the specific cell surface components crucial for the peptide-membrane interactions. A major part of the total negative surface charge of a cell is linked to various membrane-associated proteins. To investigate their possible role in the membrane permeabilization caused by PInA, the endoprotease trypsin was used to cleave extracellular parts of membrane anchored proteins protruding from the cell surface.

The effect of 10^{-4} M PInA on trypsin-treated cells was initially studied by patch clamp experiments similar to those described in Section 3.1, and Fig. 4 shows representative recordings from outside-out patches voltage clamped at -50 mV during exposure to 10^{-4} M PInA. Immediately after excision, outside-out patches were locally exposed to 25 g/L trypsin for 1 min, and the delivery pipette was removed from the dish between treatments (see Section 2.5). In contrast to the rapid development of a large inward current in untreated cells exposed to 10^{-4} M PInA (Fig. 1A), pressure ejection of 10^{-4} M PInA solved in trypsin-free solution directly onto trypsin-treated patches for more than 2 min induced no inward current (Fig. 4B). A total number of 10 trypsin-treated patches were exposed to PInA in this manner, and a pronounced inward current subsequent to the peptide application was observed in only 1 of these patches. At regular intervals during this series of experiments, control recordings were performed from 7 untreated patches, all of which responded to 10^{-4} M PInA with a large conductance increase.

Even though the trypsin-treated patches were exposed to PInA in normal, enzyme-free solution, trypsin molecules might still remain attached to the patch surface after the local pretreatment with the enzyme. In order to test if the lack of PInA-induced conductance increase was due to degradation of PInA by such remnant trypsin, similar experiments were performed using the D-enantiomeric form of PInA. The effect of trypsin on both L- and D-PInA was tested using mass spectrometry to identify intact PInA molecules and possible degradation products. Incubation of a solution with 10^{-3} M PInA

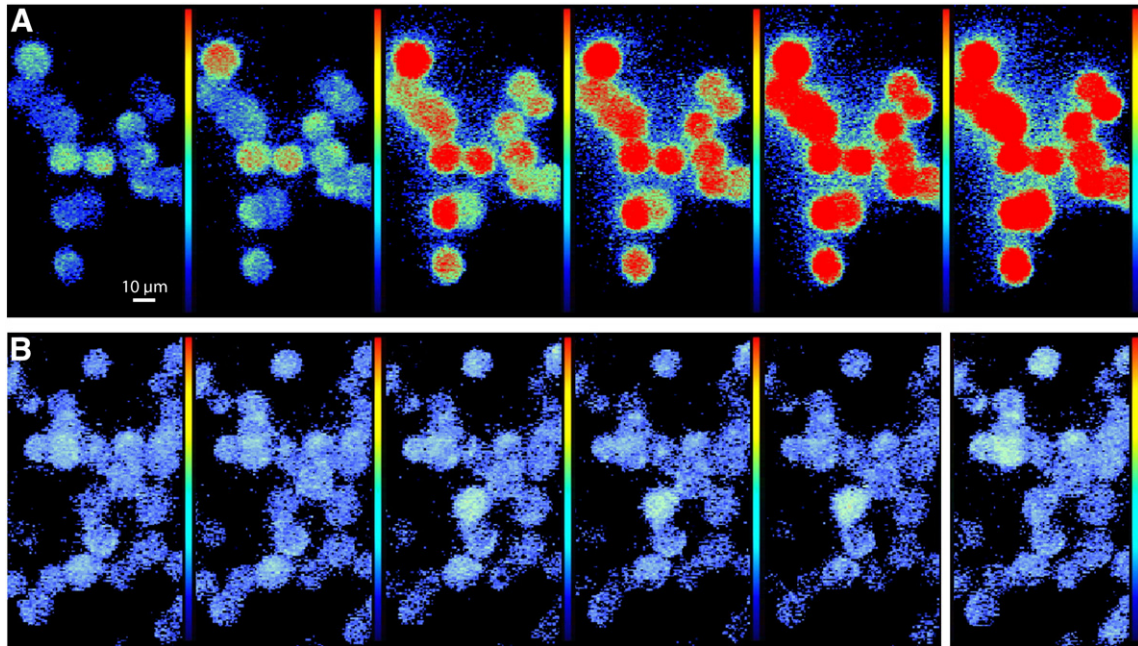


Fig. 2. Ca^{2+} imaging confirming that elevated extracellular Ca^{2+} concentration inhibits membrane permeabilization by PlnA. The images displaying the cytosolic Ca^{2+} -concentration ($[\text{Ca}^{2+}]_i$) are based on the fluorophore fura-2. Dark blue represents resting level and dark red indicates saturating levels of $[\text{Ca}^{2+}]_i$. The time interval between merged frames is 5 s and the first image in each series was taken just before start of PlnA exposure. The last, separated frame in B was taken 3 min after start of PlnA exposure. (A) Cells exposed to 10^{-4} M PlnA show a rapid increase in $[\text{Ca}^{2+}]_i$, indicating enhanced Ca^{2+} influx due to membrane permeabilization. (B) In extracellular solution with $10\times$ increased Ca^{2+} concentration (24 mM), 10^{-4} M PlnA failed to permeabilize the cell membranes.

(either L- or D-form) and 2.5 g/L trypsin showed a nearly total degradation (>95%) of the L-form after 20 min, whereas the D-form was completely resistant to degradation. We have previously shown that D-PlnA is as effective as L-PlnA in permeabilizing GH_4 cells [13], and this was verified in the present study (Fig. 4A). A total number of 9 outside-out patches from untreated cells in normal extracellular

solution were exposed to 10^{-4} M D-PlnA, and all of these patches responded in a manner similar to the one presented in Fig. 4A.

The recording in Fig. 4C is from a trypsin-treated patch exposed to D-PlnA. The holding current was virtually stable during more than 3 min continuous pressure ejection of D-PlnA onto the patch, and a similar lack of noticeable conductance increase was observed in 6 of

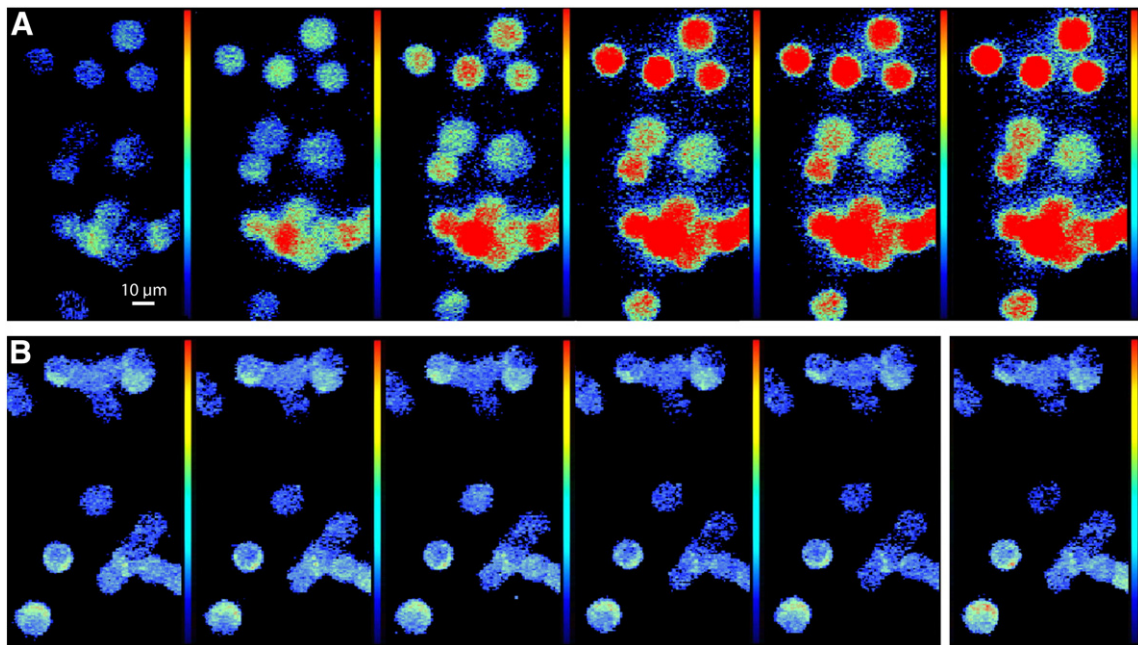


Fig. 3. Ca^{2+} imaging confirming that extracellular poly-D-lysine inhibits membrane permeabilization by PlnA. The images displaying the cytosolic Ca^{2+} -concentration ($[\text{Ca}^{2+}]_i$) are based on the fluorophore fura-2. Dark blue represents resting level and dark red indicates saturating levels of $[\text{Ca}^{2+}]_i$. The time interval between merged frames is 5 s and the first image in each series was taken just before start of PlnA exposure. The last, separated frame in B was taken 3 min after start of PlnA exposure. (A) Cells exposed to 10^{-4} M PlnA show a rapid increase in $[\text{Ca}^{2+}]_i$, indicating enhanced Ca^{2+} influx due to membrane permeabilization. (B) In solution with 5 mg/ml poly-D-lysine, 10^{-4} M PlnA failed to permeabilize the cell membranes.

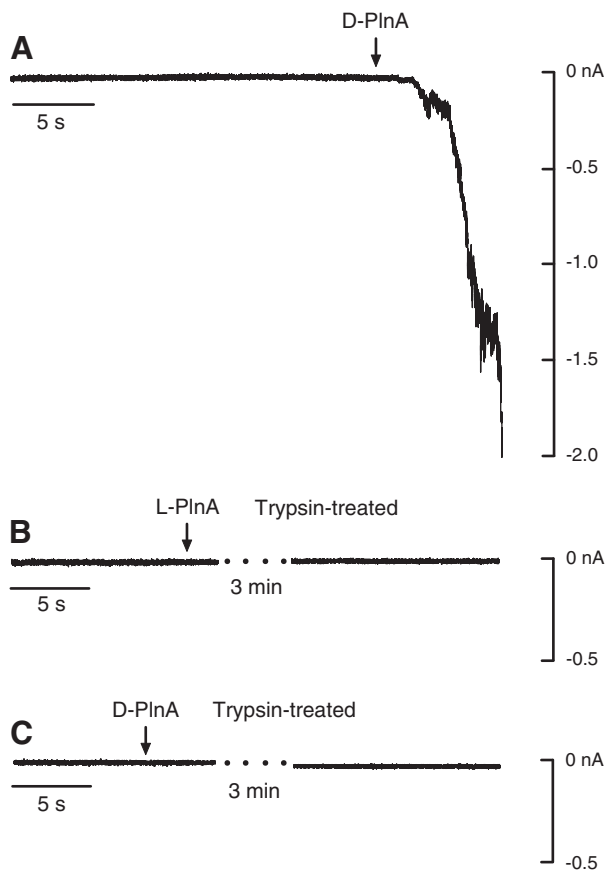


Fig. 4. Trypsin-treated membranes have reduced sensitivity to PlnA. Representative recordings from outside-out patches voltage clamped at -50 mV are displayed. Arrows indicate start of continuous pressure ejections of 10^{-4} M D-PlnA or L-PlnA onto the patches. (A) D-PlnA is as potent as L-PlnA in permeabilizing the membrane. (B) On membrane patches pretreated with 25 g/L trypsin for 1 min in order to cleave extracellular parts of membrane proteins, L-PlnA had no effect. (C) Also trypsin-resistant D-PlnA failed to permeabilize the membrane, showing that the diminished permeabilizing effect of PlnA was not due to cleavage of the peptide by membrane-associated trypsin remaining from the pretreatment.

the 8 trypsin-treated patches exposed to D-PlnA. Therefore, the increased resistance to PlnA after trypsin treatment of the patch is due to degradation of membrane associated proteins, and not to breakdown of PlnA.

It is unlikely that the lack of PlnA effects on trypsin-treated patches is due to destruction of specific membrane receptors involved in the action of PlnA, due to the similar effects of L- and D-PlnA in normal solution. A receptor-mediated mechanism could hardly be activated equally by these two enantiomeric forms of PlnA.

3.4. Microfluorometric recordings verify that trypsin-treated cells are resistant to PlnA

The conclusion based on the experiments described in the previous section was supported by microfluorometric measurements of relative $[Ca^{2+}]_i$ in trypsin-treated cells exposed to 10^{-4} M PlnA. In these experiments, the solution in the dish contained 250 mg trypsin/L, which caused the cells to partially detach from the bottom of the dish. Therefore, fluorescence changes reflecting altered $[Ca^{2+}]_i$ were measured in selected, single cells fixed by a suction micropipette. PlnA in trypsin-free solution was then applied to the selected cell by pressure ejection through a micropipette aimed at the cell, rather than flushing the cell chamber with PlnA-containing solution. In these experiments, the emission from the selected cell was measured using a photomultiplier tube, as described in Section 2.6. The

trypsin treatment used in this series of experiments is similar to the procedure employed to detach cells prior to reseeding during the cell culture. Thus, the cells stay viable and are able to undergo mitosis after incubation in the trypsin-containing solution.

Fig. 5A shows a control recording of the F360/F380 ratio, representing $[Ca^{2+}]_i$, from an untreated cell exposed to 10^{-4} M D-PlnA in normal extracellular solution. A recording of the relative emission intensity at the isosbestic excitation wavelength of 360 nm (F360), representing the cytosolic concentration of fura-2 ($[fura-2]_i$), is also included in the figure. Exposure to 10^{-4} M PlnA rapidly increased $[Ca^{2+}]_i$ to saturating levels, reflecting enhanced Ca^{2+} influx due to membrane permeabilization. Following the rapid increase in $[Ca^{2+}]_i$, a delayed and almost total loss of the large fluorophore fura-2 is evident from the trace representing $[fura-2]_i$, indicating severe disruption of the cell membrane. A total number of 25 similar control recordings were performed at regular intervals during this series of experiments, which also included 28 recordings from trypsin-treated cells. Both L-PlnA ($n=35$) and D-PlnA ($n=18$) were used in these experiments, and all the control recordings were qualitatively similar to that depicted in Fig. 5A. The two-step increase of $[Ca^{2+}]_i$ displayed in this figure may indicate a beginning recovery from the PlnA effect, before the cell was overwhelmed by the disruptive

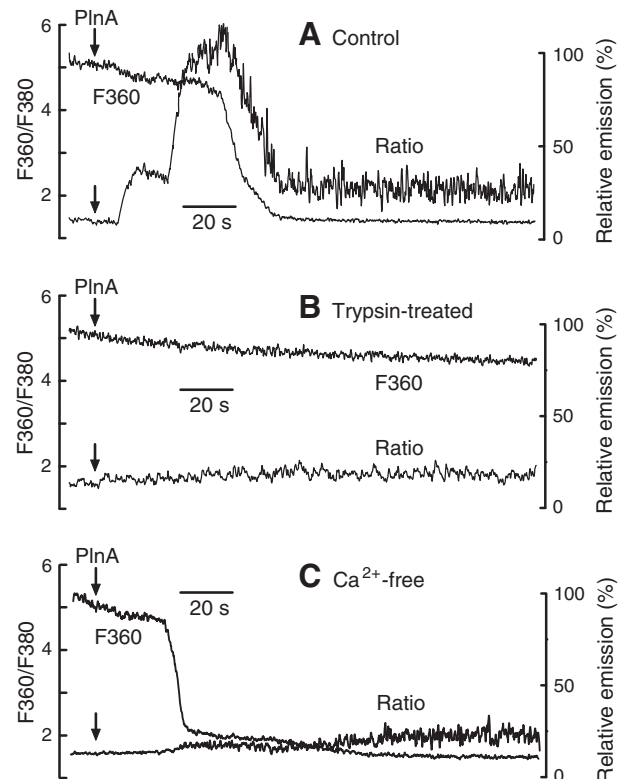


Fig. 5. Microfluorometric recordings verifying that trypsin-treated cells have reduced sensitivity to PlnA. The recordings are from single, fura-2-loaded cells exposed to PlnA. The ratio between emissions at the excitation wavelengths 360 and 380 nm (F360/F380) reflects the cytosolic Ca^{2+} concentration ($[Ca^{2+}]_i$), whereas absolute emission at the isosbestic excitation wavelength 360 nm (F360) reflects $[fura-2]_i$. Arrows indicate start of continuous pressure ejection of 10^{-4} M PlnA onto the cell. (A) In normal extracellular solution, D-PlnA elevated $[Ca^{2+}]_i$ to saturating levels followed by delayed loss of fluorophore, indicating massive membrane permeabilization. (B) Comparable recording showing lack of $[Ca^{2+}]_i$ elevation and no diffusional loss of fluorophore from a cell in solution containing 250 mg/L trypsin. Because trypsin detaches adherent cells from the bottom of the dish, the cell was fixed by a micro suction-pipette during flushing with PlnA (solved in trypsin-free solution). The presented cell was exposed to D-PlnA, but lack of $[Ca^{2+}]_i$ elevation in trypsin-containing solution was observed with both L-PlnA and D-PlnA. (C) Recording in Ca^{2+} -free solution showing lack of $[Ca^{2+}]_i$ elevation in response to PlnA application. The F360 trace reveals profound loss of fluorophore from the cytosol after a short delay, verifying that the cell was permeabilized by PlnA also in this solution. The increasing noise level of the ratio traces in A and C is due to the reduced signal to noise ratio when fluorophore is lost from the cell.

peptide action. However, a rapid and continuous elevation of $[Ca^{2+}]_i$ to the peak value was a more common response.

Fig. 5B shows representative recordings of both the F360/F380 ratio and F360 from a cell incubated in trypsin. PlnA solved in trypsin-free solution was ejected directly onto the recorded cell, which was thus superfused with trypsin-free solution during the recording. Continuous pressure ejection of 10^{-4} M D-PlnA onto the cell for more than 3 min had no effect on $[Ca^{2+}]_i$, and the modest decline of F360 was probably due to photo-bleaching rather than to diffusional loss of fura-2. In merely 4 of the 28 experiments with cells incubated in trypsin did ejection of either L-PlnA ($n=18$) or D-PlnA ($n=10$) induce elevation of $[Ca^{2+}]_i$, thus excluding the possibility that lack of PlnA effects was due to instant peptide degradation by remaining trypsin adhered to the cell surface when PlnA solved in trypsin-free solution was pressure ejected onto the cells.

In order to test the possibility that the PlnA-induced elevation of $[Ca^{2+}]_i$ in normal solution might be due to release from intracellular stores, rather than Ca^{2+} influx through a disrupted cell membrane, similar experiments were also performed in Ca^{2+} -free solution containing 0.5 mM EGTA. Fig. 5C shows a recording of the F360/F380 ratio and F360 from one of the 6 cells tested in this solution. In all the cells, PlnA failed to elevate $[Ca^{2+}]_i$, although the membrane-disruptive action of the peptide was evident from a similar diffusional loss of fura-2 as seen in normal solution. Therefore, the elevation of $[Ca^{2+}]_i$ induced by PlnA in normal solution is due to influx of extracellular Ca^{2+} .

Based on the data from both the patch clamp and the microfluorometric recordings, it is reasonable to conclude that membrane-associated proteins are important for the membrane-permeabilizing effect of PlnA.

3.5. Removal of carbohydrate residues from glycosylated membrane proteins prevents membrane permeabilization by PlnA

The reduced membrane sensitivity to PlnA induced by trypsin treatment does not reveal which parts of the membrane-associated proteins that are involved in the PlnA-membrane interactions. The experiments described in Sections 3.1–2 demonstrate that negative surface charge of the cell membrane is probably important for the membrane-permeabilizing effect of PlnA. Several types of carbohydrate residues linked to the protein backbone of membrane-associated glycoproteins and proteoglycans carry negative charges. For example, the glycosaminoglycans linked to the protein core of proteoglycans are negatively charged because of the prevalence of sulphate groups. In an attempt to identify molecular groups involved in mediating the membrane-permeabilizing effect of PlnA, cells were exposed to a mixture of enzymes that cleave carbohydrate residues from protein backbones, i.e., PNGase F, chondroitinase ABC, and heparinase I, II, III.

The effect of 10^{-4} M PlnA on cells treated with the enzyme mixture specified in Section 2.4 for 2–3 h was initially studied by patch clamp experiments similar to those described in Section 3.1. Cells incubated with the enzyme mixture according to the described protocol stayed viable in culture, and kept their ability of mitotic cell division. Contrary to the inward current rapidly induced by 10^{-4} M PlnA in outside-out patches from untreated cells (Fig. 6A), exposure to 10^{-4} M PlnA for more than 2 min induced no detectable inward current in the outside-out patch from the enzyme-treated cell presented in Fig. 6B. This recording started about 5 min after replacement of the enzyme solution in the dish with normal extracellular solution, and a total number of 7 patches from cells treated with the enzyme mixture were exposed to 10^{-4} M PlnA within one hour after wash-out of the enzyme-containing solution. A prominent inward current subsequent to PlnA exposure was observed in only 1 of these patches. At regular intervals during this series of experiments, 4 control recordings were performed from sham-treated cells of the same seeding. The same procedures were then followed regarding solution changes, incubation period, and timing of the recordings, but

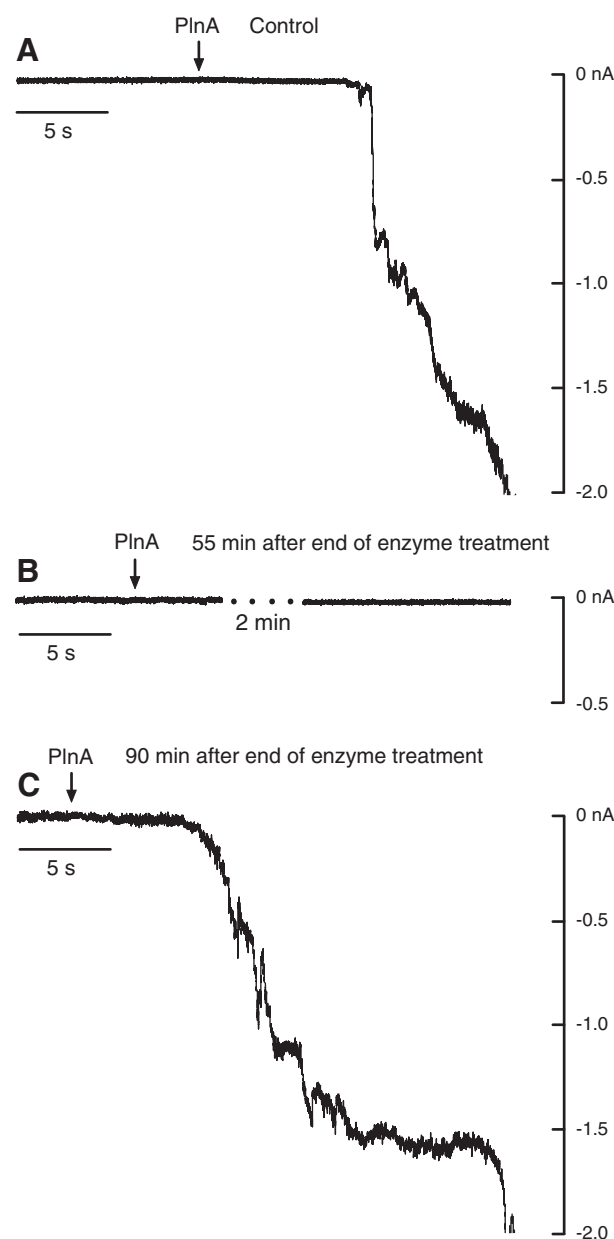


Fig. 6. Carbohydrate removal from glycosylated membrane proteins inhibits membrane permeabilization by PlnA. Representative recordings from outside-out patches voltage clamped at -50 mV are displayed. Arrows indicate start of continuous pressure ejections of 10^{-4} M PlnA onto the patches. (A) Control recording showing the permeabilizing effect of PlnA. (B) In patches from cells pre-exposed to a mixture of enzymes that split carbohydrate residues from the backbone of proteins, PlnA failed to permeabilize the membrane. (C) After a period of about 1.5 h in normal extracellular solution, the enzyme-treated cells regained their sensitivity to PlnA.

only normal extracellular solution was applied. In all of the control recordings, 10^{-4} M PlnA induced a pronounced inward current (Fig. 6A).

In live cells, there is a constant turnover of membrane associated proteins and their carbohydrate side chains. Thus, when the enzyme-containing solution was replaced with normal extracellular solution, it was to be expected that normal membrane composition would gradually be reestablished. Indeed, Fig. 6C shows a representative recording from a patch excised from a cell 1.5 h after removal of the solution containing the enzyme mixture, and it is evident that the cell had regained its sensitivity to PlnA during this period. Among the 10 patches excised between 1 h and 2 h after exchange of the test solution with normal extracellular solution, 10^{-4} M L-PlnA induced a pronounced inward current in 6 patches. All the 8 patches excised more than 2 h

after termination of the enzyme treatment were rapidly permeabilized by 10^{-4} M PInA.

3.6. Ca^{2+} imaging confirms that the effect of PInA is dependent on glycosylated proteins

The results from the patch-clamp experiments presented above were verified by Ca^{2+} imaging experiments similar to those described in Section 3.2. Fig. 7A depicts a control recording from sham-treated cells, and shows that all cells in the field of view displayed an apparent color shift representing a rapid increase of $[Ca^{2+}]_i$ less than 5 s after exposure to 10^{-4} M PInA. After 20–25 s, most cells had reached saturating levels of $[Ca^{2+}]_i$. Fig. 7B presents a recording from cells of the same seeding incubated with enzyme mixture for 2 h, and 10 min after replacement of the enzyme-containing solution with normal extracellular solution. As opposed to the obviously increased $[Ca^{2+}]_i$ in the control cells (Fig. 7A), the $[Ca^{2+}]_i$ of cells pre-treated with the enzyme mixture was seemingly quite stable, even after 3 min exposure to 10^{-4} M PInA.

This series of experiments comprised 4 dishes with cells pre-treated with the enzyme mixture less than 50 min prior to the recording. The control recordings from sham-treated dishes were performed at regular intervals in order to test the potency of 10^{-4} M PInA on cells from this particular seeding. In all the 3 control dishes, the cells displayed pronounced elevation of $[Ca^{2+}]_i$ within less than 30 s in response to 10^{-4} M PInA. In the control experiments, the F340/F380 ratio of the observed cells increased by a factor of 4.4 ± 1.2 ($n=50$) after 30 s exposure to 10^{-4} M PInA. However, when pretreated with the enzyme mixture, the F340/F380 ratio of the recorded cells increased by a factor of only 1.1 ± 1.1 ($n=80$) after 3 min exposure to 10^{-4} M PInA. This difference in ratio increase between the sham-treated and enzyme-treated cells is highly significant ($p<0.0001$). Probably due to strain

on the cells exerted by the combination of the fura-2 loading procedure and the enzyme treatment for more than 2 h, the cells started to detach from the bottom of the dish before 1 h after wash-out of the enzyme mixture. Therefore, we were not able to verify by Ca^{2+} imaging that the enzyme-treated cells started to regain their sensitivity to PInA after about 1 h in normal extracellular solution.

4. Discussion

It is generally assumed that electrostatic attraction to negatively charged phospholipids initiates permeabilization of cell membranes by cationic and amphiphilic antimicrobial peptides, but other factors may also be essential in this process. Negatively charged phospholipids are more abundant in the inner leaflet than in the outer leaflet of eukaryotic cell membranes, but we have previously shown that the membrane is permeabilized less readily by PInA if the inner leaflet is exposed to the peptide [12,13]. Therefore, we suggested that anionic phospholipids alone cannot explain the peptide-membrane interaction [13], and that negatively charged membrane proteins may be essential for the lytic effect of PInA.

In the present study, we showed that the permeabilizing potency of PInA diminished in extracellular solutions that partially neutralize negative cell surface charge. Although these results are compatible with the notion that electrostatic attraction is involved in the permeabilization mechanism, they are not definite proof of such a mechanism. For example, Ca^{2+} and polyvalent cationic poly-D-lysine may also have a stabilizing effect on the membrane by bridging anionic groups of various membrane constituents. The involvement of membrane proteins in PInA's action on the membrane was demonstrated by the impeded lytic potency of the peptide after enzymatic removal of extracellular regions of membrane proteins or their carbohydrate residues. However, the membrane permeabilization of eukaryotic

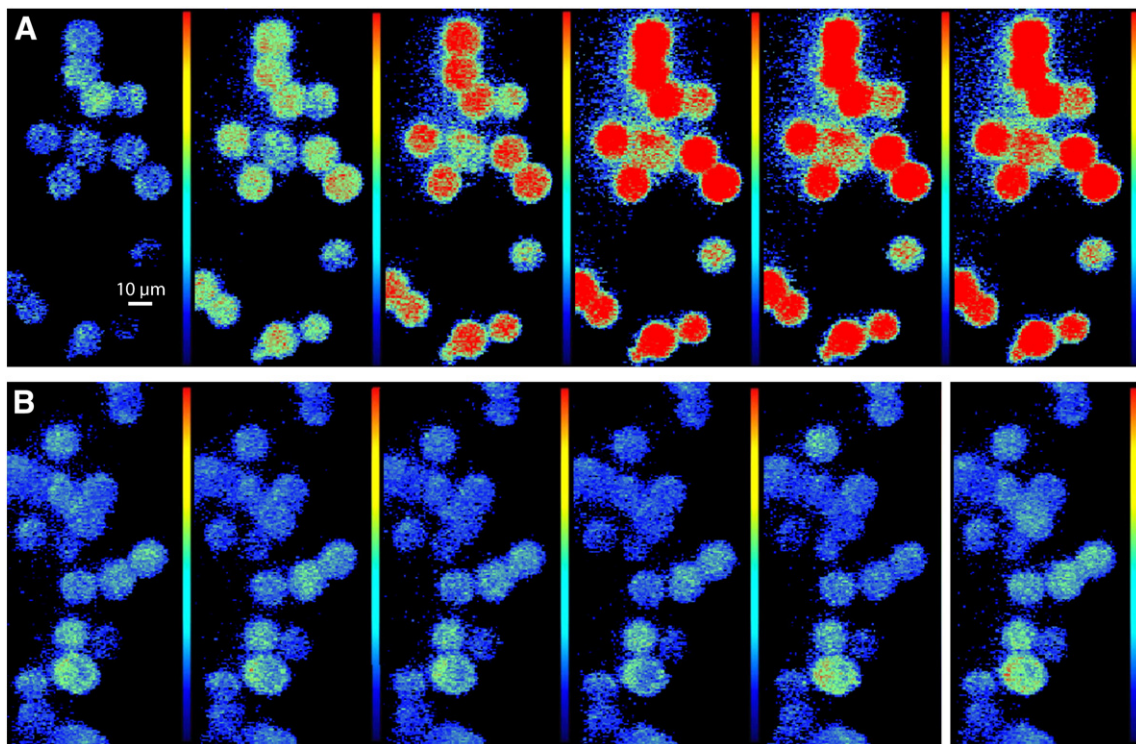


Fig. 7. Ca^{2+} imaging confirming the dependence of glycosylated membrane proteins for the effect of PInA. The images displaying the cytosolic Ca^{2+} -concentration ($[Ca^{2+}]_i$) are based on the fluorophore fura-2. Dark blue represents resting level and dark red indicates saturating levels of $[Ca^{2+}]_i$. Time interval between merged frames is 5 s and the first image in each series was taken just before start of PInA exposure. The last, separated frame in B was taken 3 min after start of PInA exposure. (A) Control recording of elevated $[Ca^{2+}]_i$ induced by 10^{-4} M PInA, indicating membrane permeabilization. (B) In cells pre-exposed to a mixture of enzymes that split carbohydrate residues from the backbone of proteins, PInA failed to permeabilize the membrane.

cells by cationic and amphiphilic antimicrobial peptides may not necessarily be facilitated by negatively charged membrane proteins. If this attraction is sufficiently strong to prevent dissociation of the peptide and its subsequent insertion into the lipid bilayer, the membrane proteins may instead function as a screen that protects the cell against the lytic effect of the peptide. Such a screening mechanism has recently been described by Fadnes et al. [53] for the peptides bovine lactoferrin and a designer peptide, but the same group has later shown that surface-bound heparan sulfate may enhance the lytic effect of small peptides [54]. Furthermore, eukaryotic cell membrane penetration by a 22-mer peptide derived from human lactoferrin is dependent on initial binding to heparan sulfate [55]. Thus, the consequences of the interference between glycosylated membrane proteins and lytic peptides seem to depend on the properties of the peptide, and range from protection against lysis to facilitation of the membrane permeabilizing effect.

The figures presented in Section 3 may give the impression that neutralizing negative cell surface charge or cleaving off extracellular parts of membrane proteins or their carbohydrate residues render the cells completely resistant to PlnA. However, this may of course not be the case. In a previous flow-cytometric study of the effect of PlnA on the integrity of both normal and transformed lymphocytes, we showed that the dose–response relationship for the membrane-disrupting effect of PlnA is very steep, with a ratio of about 5 between the lowest concentration permeabilizing virtually all the cells and a concentration that has no detectable effect [13]. Therefore, PlnA at a concentration inducing a full-fledged response in control cells may be completely ineffective subsequent to cell treatments that merely reduce the sensitivity of the cells to PlnA. A possible right-shift of the dose–response relationship for the effect of PlnA might have been revealed by testing higher concentrations of the peptide. However, the main objective of the present study was to demonstrate possible involvement of negatively charged membrane proteins in the PlnA-induced membrane permeabilization, and not to establish post-treatment dose–response curves for the PlnA effect.

In order to test if glycosylated membrane proteins facilitate PlnA-induced membrane permeabilization, we employed a mixture of the enzymes chondroitinase ABC, heparinase I, II, III, and N-Glycosidase F to cleave off various carbohydrate residues from membrane proteins. The chondroitinases cleave various chondroitins, the most prevalent of all the glycosaminoglycans, while the heparinases are active toward both heparan sulfate and heparin, which has the highest negative charge density of any known biological molecule. N-Glycosidase F catalyses hydrolysis of numerous N-linked glycans. Obviously, treatment with this enzyme mixture is not very specific, but rids the membrane-associated proteins of the most significant negatively charged carbohydrate residues. It would of course be interesting to scrutinize the relative importance of the various carbohydrate groups, which could be achieved by applying the enzymes individually and in different combinations. The involvement of the various carbohydrate residues are probably not all-or-none, and the use of specific enzyme treatment to resolve the relative importance of the different groups is likely to be rather extensive and the results difficult to interpret. Such experiments are beyond the main objective of the present project, but should be included in future studies.

Interestingly, the protecting effect of the enzyme mixture was transient. Between 1 and 2 h after replacement of the enzyme-containing solution with normal extracellular solution, cells gradually became susceptible to PlnA. In the same dish, cells regained their sensitivity with different delays, but after 2 h, virtually all cells were permeabilized when exposed to PlnA. Live cells continuously synthesize glycoproteins and proteoglycans that are inserted in the cell membrane. The time window within which the cells regained sensitivity to PlnA after enzyme treatment may thus reflect the turnover rate of glycosylated membrane proteins in the GH₄ cell line. The regained PlnA sensitivity observed after removing the enzyme mixture also indicates that the

cells stayed viable during the enzyme treatment and experimental procedures.

It is well established that the density of negatively charged phospholipids in the outer membrane leaflet in cancer cells is increased relative to that of normal, healthy cells [37–40], and the composition of membrane-associated macromolecules is also different in normal and cancerous cells. The expression of proteoglycans and the selection of carbohydrate moieties of glycoproteins change significantly through neoplastic transformation in malignancies such as lung carcinoma, ovarian cancer, osteosarcoma, brain tumors, mesothelioma, colon cancer, breast cancer and pancreatic cancer [41–48]. Such alterations of the glycocalyx, and not only the increased density of negatively charged phospholipids, may explain why some antimicrobial peptides at certain concentrations preferentially lyse and kill cancerous eukaryotic cells, whereas their normal counterparts are not affected. Initial interaction with membrane- or cell wall-associated carbohydrates is also essential for the effect of many antimicrobial peptides on their natural target cells, bacteria [56].

Cationic antimicrobial peptides are promising novel agents for cancer treatment [57], and our initial report of selective permeabilization of cancerous pituitary cells by PlnA was encouraging regarding a possible clinical potential of the peptide [13]. However, it turned out that normal rodent neurons, human lymphocytes, and various cancerous counterparts of these cell types were permeabilized by PlnA at about the same concentration of the peptide [14]. Normal rat liver cells (hepatocytes, endothelial cells, and Kupffer cells) and renal epithelial cells were also permeabilized by PlnA [12]. Thus, the permeabilizing effect of PlnA on eukaryotic cells is not restricted to cancerous cells. The literature on the lytic effect of antimicrobial peptides on cancer cells includes several preliminary, promising reports not corroborated by subsequent publications, which may imply that also other antimicrobial peptides have turned out to be less selective for cancer cells than indicated by the initial studies. Many attempts at designing peptides with improved selectivity and potency regarding anti-tumor properties have been made (reviewed in [11]), but their success has so far been limited.

However, the notion that high selectivity for tumor cells is crucial for application of antimicrobial peptides in cancer treatment has recently been challenged. Local lysis of tumor cells by oncolytic viruses may activate a systemic immune response selective for cells from the same clone as the lysed cells [21,22], and Berge et al. [20] have demonstrated that local lysis of tumor cells by a lytic peptide derived from lactoferrin induces a similar, selective immune response. In a series of experiments, both T cell-deficient and immunocompetent mice were inoculated with murine lymphoma cells, and, when solid tumors had formed, the lytic peptide was injected intratumorally. This treatment induced significant inhibition of tumor growth in all the animals. Interestingly, complete tumor regression and no recurrence was observed in a majority of the immunocompetent mice, whereas tumor regression was only transient in the T cell-deficient individuals. Moreover, upon reinoculating mice in which tumors had been completely eradicated, renewed tumor growth was sparse and complete regression of the tumors occurred without treatment. In contrast, a different syngenic tumor-forming cell line readily established lethal tumors when inoculated in mice previously cured of the lymphoma. These results suggest that lytic peptides may induce specific immunity through spillage of antigens from the lysed cells, thereby rendering the host impervious to reestablishment of tumors by cells from the same clone as the lysed cells.

Because local lysis of cancer cells may activate a specific, systemic immune response, and thus initiate an attack on both the injected tumor and recurrences, strong selectivity for cancer cells is not a prerequisite for a lytic peptide to have therapeutic potential. However, local administration of a non-specific lytic peptide faces many of the same challenges as irradiation- and surgical cancer therapy, e.g., severe damage of adjacent healthy tissue. The very steep dose–response curve of PlnA is particularly interesting in this regard [12–14]. By

intra-tumoral injection of PlnA, it is feasible to reach a local peptide concentration sufficient to rapidly permeabilize cancer cells, while the level of PlnA in the bordering regions will be too low to influence cell membrane integrity. Therefore, the therapeutic potential of PlnA and similar peptides may be considerable.

We conclude that electrostatic attraction to not only negatively charged phospholipids, but also to glycosylated membrane proteins is probably involved in the PlnA-induced membrane permeabilization of eukaryotic cells. We envisage that the attraction to negatively charged membrane proteins is a necessary first step, in order for PlnA to reach a sufficiently high concentration close to the lipid bilayer for the next step to occur, i.e., interaction with negatively charged phospholipids and insertion into the outer leaflet of the lipid bilayer. The involvement of specific carbohydrate residues in this process and the possible therapeutic potential of PlnA and similar peptides should be investigated in future studies.

Acknowledgements

We are grateful to Kristian Prydz for valuable discussions and for providing the various enzymes, and to Kirsten Ore for assistance with the cell cultures.

References

- [1] H.M. Chen, K.W. Leung, N.N. Thakur, A. Tan, R.W. Jack, Distinguishing between different pathways of bilayer disruption by the related antimicrobial peptides cecropin B, B1 and B3, *Eur. J. Biochem.* 270 (2003) 911–920.
- [2] G. Fimland, L. Johnsen, B. Dalhus, J. Nissen-Meyer, Pediocin-like antimicrobial peptides (class IIa bacteriocins) and their immunity proteins: biosynthesis, structure, and mode of action, *J. Pept. Sci.* 11 (2005) 688–696.
- [3] J. Nissen-Meyer, I.F. Nes, Ribosomally synthesized antimicrobial peptides: their function, structure, biogenesis, and mechanism of action, *Arch. Microbiol.* 167 (1997) 67–77.
- [4] M. Zasloff, Antimicrobial peptides of multicellular organisms, *Nature* 415 (2002) 389–395.
- [5] H.M. Chen, W. Wang, D. Smith, S.C. Chan, Effects of the anti-bacterial peptide cecropin B and its analogs, cecropins B-1 and B-2, on liposomes, bacteria, and cancer cells, *Biochim. Biophys. Acta* 1336 (1997) 171–179.
- [6] J.S. Ye, X.J. Zheng, K.W. Leung, H.M. Chen, F.S. Sheu, Induction of transient ion channel-like pores in a cancer cell by antibiotic peptide, *J. Biochem.* 136 (2004) 255–259.
- [7] R.A. Cruciani, J.L. Barker, M. Zasloff, H.C. Chen, O. Colamonic, Antibiotic magainins exert cytolytic activity against transformed cell lines through channel formation, *Proc. Natl. Acad. Sci. U. S. A.* 88 (1991) 3792–3796.
- [8] L. Jacob, M. Zasloff, Potential therapeutic applications of magainins and other antimicrobial agents of animal origin, *Ciba Found. Symp.* 186 (1994) 197–216.
- [9] R.I. Lehrer, A.K. Lichtenstein, T. Ganz, Defensins: antimicrobial and cytotoxic peptides of mammalian cells, *Annu. Rev. Immunol.* 11 (1993) 105–128.
- [10] A. Lichtenstein, Mechanism of mammalian cell lysis mediated by peptide defensins. Evidence for an initial alteration of the plasma membrane, *J. Clin. Invest.* 88 (1991) 93–100.
- [11] C. Leuschner, W. Hansel, Membrane disrupting lytic peptides for cancer treatments, *Curr. Pharm. Des.* 10 (2004) 2299–2310.
- [12] K. Andersland, G.F. Jolle, O. Sand, T.M. Haug, Peptide pheromone plantaricin A produced by *Lactobacillus plantarum* permeabilizes liver and kidney cells, *J. Membr. Biol.* 235 (2010) 121–129.
- [13] S.L. Sand, T.M. Haug, J. Nissen-Meyer, O. Sand, The bacterial peptide pheromone plantaricin A permeabilizes cancerous, but not normal, rat pituitary cells and differentiates between the outer and inner membrane leaflet, *J. Membr. Biol.* 216 (2007) 61–71.
- [14] S.L. Sand, C. Oppegard, S. Ohara, T. Iijima, S. Naderi, H.K. Blomhoff, J. Nissen-Meyer, O. Sand, Plantaricin A, a peptide pheromone produced by *Lactobacillus plantarum*, permeabilizes the cell membrane of both normal and cancerous lymphocytes and neuronal cells, *Peptides* 31 (2010) 1237–1244.
- [15] D.B. Diep, L.S. Havarstein, J. Nissen-Meyer, I.F. Nes, The gene encoding plantaricin A, a bacteriocin from *Lactobacillus plantarum* C11, is located on the same transcription unit as an agr-like regulatory system, *Appl. Environ. Microbiol.* 60 (1994) 160–166.
- [16] H.H. Hauge, D. Mantzilas, G.N. Moll, W.N. Konings, A.J. Driessen, V.G. Eijsink, J. Nissen-Meyer, Plantaricin A is an amphiphilic alpha-helical bacteriocin-like pheromone which exerts antimicrobial and pheromone activities through different mechanisms, *Biochemistry* 37 (1998) 16026–16032.
- [17] E.L. Anderssen, D.B. Diep, I.F. Nes, V.G. Eijsink, J. Nissen-Meyer, Antagonistic activity of *Lactobacillus plantarum* C11: two new two-peptide bacteriocins, plantaricins EF and JK, and the induction factor plantaricin A, *Appl. Environ. Microbiol.* 64 (1998) 2269–2272.
- [18] H. Zhao, R. Sood, A. Jutila, S. Bose, G. Fimland, J. Nissen-Meyer, P.K. Kinnunen, Interaction of the antimicrobial peptide pheromone plantaricin A with model membranes: implications for a novel mechanism of action, *Biochim. Biophys. Acta* 1758 (2006) 1461–1474.
- [19] P.E. Kristiansen, G. Fimland, D. Mantzilas, J. Nissen-Meyer, Structure and mode of action of the membrane-permeabilizing antimicrobial peptide pheromone plantaricin A, *J. Biol. Chem.* 280 (2005) 22945–22950.
- [20] G. Berge, L.T. Eliassen, K.A. Camilio, K. Bartnes, B. Sveinbjornsson, O. Rekdal, Therapeutic vaccination against a murine lymphoma by intratumoral injection of a cationic anticancer peptide, *Cancer Immunol.* 59 (2010) 1285–1294.
- [21] P. Marcatò, C.A. Dean, C.A. Giacomantonio, P.W. Lee, Oncolytic reovirus effectively targets breast cancer stem cells, *Mol. Ther.* 17 (2009) 972–979.
- [22] P. Hunter, The fourth front against cancer. The first clinical trials to test engineered viruses that attack tumour cells have yielded promising results for future cancer therapies, *EMBO Rep.* 12 (2011) 769–771.
- [23] R.E. Hancock, D.S. Chapple, Peptide antibiotics, *Antimicrob. Agents Chemother.* 43 (1999) 1317–1323.
- [24] K. Matsuzaki, Magainins as paradigm for the mode of action of pore forming poly-peptides, *Biochim. Biophys. Acta* 1376 (1998) 391–400.
- [25] Z. Oren, Y. Shai, Mode of action of linear amphipathic alpha-helical antimicrobial peptides, *Biopolymers* 47 (1998) 451–463.
- [26] Y. Shai, Mode of action of membrane active antimicrobial peptides, *Biopolymers* 66 (2002) 236–248.
- [27] A. Tossi, L. Sandri, A. Giangaspero, Amphipathic, alpha-helical antimicrobial peptides, *Biopolymers* 55 (2000) 4–30.
- [28] I. Zelezetsky, S. Pacor, U. Pag, N. Papo, Y. Shai, H.G. Sahl, A. Tossi, Controlled alteration of the shape and conformational stability of alpha-helical cell-lytic peptides: effect on mode of action and cell specificity, *Biochem. J.* 390 (2005) 177–188.
- [29] B. Bechinger, Rationalizing the membrane interactions of cationic amphipathic antimicrobial peptides by their molecular shape, *Curr. Opin. Colloid Interface* 14 (2009) 349–355.
- [30] B. Bechinger, Insights into the mechanisms of action of host defence peptides from biophysical and structural investigations, *J. Pept. Sci.* 17 (2011) 306–314.
- [31] A. Marquette, A.J. Mason, B. Bechinger, Aggregation and membrane permeabilizing properties of designed histidine-containing cationic linear peptide antibiotics, *J. Pept. Sci.* 14 (2008) 488–495.
- [32] K. Balasubramanian, A.J. Schroit, Aminophospholipid asymmetry: a matter of life and death, *Annu. Rev. Physiol.* 65 (2003) 701–734.
- [33] K. Matsuzaki, K. Sugishita, N. Fujii, K. Miyajima, Molecular basis for membrane selectivity of an antimicrobial peptide, magainin 2, *Biochemistry* 34 (1995) 3423–3429.
- [34] K. Matsuzaki, Why and how are peptide-lipid interactions utilized for self-defense? Magainins and tachyplelins as archetypes, *Biochim. Biophys. Acta* 1462 (1999) 1–10.
- [35] Y. Shai, Mechanism of the binding, insertion and destabilization of phospholipid bilayer membranes by alpha-helical antimicrobial and cell non-selective membrane-lytic peptides, *Biochim. Biophys. Acta* 1462 (1999) 55–70.
- [36] S. Castano, B. Desbat, A. Delfour, J.M. Dumas, A. da Silva, J. Dufourcq, Study of structure and orientation of mesentericin Y105, a bacteriocin from Gram-positive *Leuconostoc mesenteroides*, and its Trp-substituted analogues in phospholipid environments, *Biochim. Biophys. Acta* 1668 (2005) 87–98.
- [37] T. Utsugi, A.J. Schroit, J. Connor, C.D. Bucana, I.J. Fidler, Elevated expression of phosphatidylserine in the outer membrane leaflet of human tumor cells and recognition by activated human blood monocytes, *Cancer Res.* 51 (1991) 3062–3066.
- [38] L.V. Rao, J.F. Tait, A.D. Hoang, Binding of annexin V to a human ovarian carcinoma cell line (OC-2008). Contrasting effects on cell surface factor VIIa/tissue factor activity and prothrombinase activity, *Thromb. Res.* 67 (1992) 517–531.
- [39] M. Sugimura, R. Donato, V.V. Kakkar, M.F. Scully, Annexin V as a probe of the contribution of anionic phospholipids to the procoagulant activity of tumour cell surfaces, *Blood Coagul. Fibrinolysis* 5 (1994) 365–373.
- [40] P. Williamson, R.A. Schlegel, Back and forth: the regulation and function of transbilayer phospholipid movement in eukaryotic cells, *Mol. Membr. Biol.* 11 (1994) 199–216.
- [41] R.V. Iozzo, R.P. Bolender, T.N. Wight, Proteoglycan changes in the intercellular matrix of human colon carcinoma: an integrated biochemical and stereologic analysis, *Lab. Invest.* 47 (1982) 124–138.
- [42] J. Kleeff, T. Ishiwata, A. Kumbasar, H. Friess, M.W. Buchler, A.D. Lander, M. Korc, The cell-surface heparan sulfate proteoglycan glypican-1 regulates growth factor action in pancreatic carcinoma cells and is overexpressed in human pancreatic cancer, *J. Clin. Invest.* 102 (1998) 1662–1673.
- [43] K. Matsuda, H. Maruyama, F. Guo, J. Kleeff, J. Itakura, Y. Matsumoto, A.D. Lander, M. Korc, Glypican-1 is overexpressed in human breast cancer and modulates the mitogenic effects of multiple heparin-binding growth factors in breast cancer cells, *Cancer Res.* 61 (2001) 5562–5569.
- [44] B.P. Toole, T.N. Wight, M.I. Tammi, Hyaluronan-cell interactions in cancer and vascular disease, *J. Biol. Chem.* 277 (2002) 4593–4596.
- [45] C.Y. Fears, C.L. Gladson, A. Woods, Syndecan-2 is expressed in the microvasculature of gliomas and regulates angiogenic processes in microvascular endothelial cells, *J. Biol. Chem.* 281 (2006) 14533–14536.
- [46] C.Y. Fears, A. Woods, The role of syndecans in disease and wound healing, *Matrix Biol.* 25 (2006) 443–456.
- [47] S. Muniese, Y. Kusano, K. Oguri, N. Itano, Y. Yoshitomi, H. Nakanishi, I. Yamashina, M. Okayama, The role of syndecan-2 in regulation of actin-cytoskeletal organization of Lewis lung carcinoma-derived metastatic clones, *Biochem. J.* 363 (2002) 201–209.
- [48] H. Park, Y. Kim, Y. Lim, I. Han, E.S. Oh, Syndecan-2 mediates adhesion and proliferation of colon carcinoma cells, *J. Biol. Chem.* 277 (2002) 29730–29736.

- [49] A.D. Theocharis, D.A. Theocharis, High-performance capillary electrophoretic analysis of hyaluronan and galactosaminoglycan-disaccharides in gastrointestinal carcinomas. Differential disaccharide composition as a possible tool-indicator for malignancies, *Biomed. Chromatogr.* 16 (2002) 157–161.
- [50] A.D. Theocharis, M.E. Tsara, N. Papageorgacopoulou, D.D. Karavias, D.A. Theocharis, Pancreatic carcinoma is characterized by elevated content of hyaluronan and chondroitin sulfate with altered disaccharide composition, *Biochim. Biophys. Acta* 1502 (2000) 201–206.
- [51] M.E. Tsara, N. Papageorgacopoulou, D.D. Karavias, D.A. Theocharis, Distribution and changes of glycosaminoglycans in neoplasias of rectum, *Anticancer Res.* 15 (1995) 2107–2112.
- [52] A.H. Tashjian Jr., Y. Yasumura, L. Levine, G.H. Sato, M.L. Parker, Establishment of clonal strains of rat pituitary tumor cells that secrete growth hormone, *Endocrinology* 82 (1968) 342–352.
- [53] B. Fadnes, O. Rekdal, L. Uhlin-Hansen, The anticancer activity of lytic peptides is inhibited by heparan sulfate on the surface of the tumor cells, *BMC Cancer* 9 (2009) 183.
- [54] B. Fadnes, L. Uhlin-Hansen, I. Lindin, O. Rekdal, Small lytic peptides escape the inhibitory effect of heparan sulfate on the surface of cancer cells, *BMC Cancer* 11 (2011) 116.
- [55] F. Duchardt, I.R. Ruttekolk, W.P.R. Verdurmen, H. Lortat-Jacob, J. Burck, H. Hufnagel, R. Fischer, M. van den Heuvel, D.W.P.M. Lowik, G.W. Vuister, A. Ulrich, M. de Waard, R. Brock, A cell-penetrating peptide derived from human lactoferrin with conformation-dependent uptake efficiency, *J. Biol. Chem.* 284 (2009) 36099–36108.
- [56] M.R. Yeaman, N.Y. Yount, Mechanisms of antimicrobial peptide action and resistance, *Pharmacol. Rev.* 55 (2003) 27–55.
- [57] J.S. Mader, D.W. Hoskin, Cationic antimicrobial peptides as novel cytotoxic agents for cancer treatment, *Exp. Opin. Investig. Drugs* 15 (2006) 933–946.